https://doi.org/10.5194/egusphere-2025-625
Preprint. Discussion started: 5 March 2025

Spatiotemporal Evaluation of Vertical Dynamics Propagation of Flash Drought and Driving Mechanisms in the Indus Basin in South Asia (1970-2023)

Tahira Khurshid[1], Qiongfang Li[1,2], Chuanhao Wu[2], Akif Rahim[3], Muhammad Shafeeque[4,5,6], Shanshui Yuan[2], Zia Ul Hassan[7], Junliang Jin[2,8,9]

1College of Hydrology and Water Resources, Hohai University, 210098 Nanjing, China

2The National Key Laboratory of Water Disaster Prevention, Hohai University, 210098 Nanjing, China

3International Water Management Institute, 53700 Lahore, Pakistan

4Climate Lab, Institute of Geography, University of Bremen, 28359 Bremen Germany

5Alfred Wegener Institute (AWI), Helmholtz Centre for Polar and Marine Research, 27570 Bremerhaven, Germany

6MARUM - Center for Marine Environmental Sciences, University of Bremen, 28359 Bremen Germany

7Department of Hydraulic Engineering, Tsinghua University, 100190 Beijing, China

8Yangtze Institute for Conservation and Development, Nanjing 210098, China

9Research Centre for Climate Change of Ministry of Water Resources, Nanjing 210029, China

Corresponding authors: Qiongfang Li (qfli@hhu.edu.cn) & Chuanhao Wu (wuch0907@hotmail.com)

Abstract

Flash drought (FD) leads to relatively short periods of anomalously low and rapid decreasing soil moisture (*SM*), which can significantly affect vegetation growth and ecosystem. However, the vertical propagation characteristics and driving mechanisms of FD through soil columns remain largely unknown, which is crucial for guiding agricultural and ecological disaster prevention and reduction. Here, we present a multi-layer FD evaluation method to explore the vertical propagation of FD at different soil depths (0-10 cm, 10-40 cm, and 100 cm), and based on the GLDAS data we comprehensively evaluate the spatiotemporal dynamics and driving mechanisms of FD during 1970-2023 in the Indus Basin, a highly climate-sensitive region. We find that the frequency of FD decreases with increasing soil depth, while the relationship between the rate of intensification (*RI*) and drought severity varies with soil depth, with stronger correlation (r^2>0.9) in the middle and root zone soil layers than in the upper layer. We further identify 2148 simultaneous events ('*t*') and 1154 subsequent events ('*t*+1') between the upper and middle soil layers, which mostly occur during spring and early summer. The temporal differences in the '*t*+1' FD events are closely related to the persistence of meteorological conditions. In contrast, the '*t*' events are caused by the simultaneous depletion of *SM* from the upper layer to the deeper layer, indicating the rapid development of FD conditions due to deeper moisture loss. The analysis also highlights the significant spatial heterogeneity of FD characteristics, with the humid and sub-humid regions in the middle Indus basin being the most sensitive to FD, and precipitation deficit and high temperature are the dominant driving forces for FD occurrence.

https://doi.org/10.5194/egusphere-2025-625
Preprint. Discussion started: 5 March 2025

Key words: Flash drought, rate of intensification, soil moisture anomalies, vertical propagation, GLDAS, Indus basin.

1 Introduction

Drought is a complex hydrometeorological phenomenon with far-reaching impacts on agriculture, water resources, and ecosystems (Mishra et al., 2010). Among various drought types, flash drought (FD) has emerged as a critical area of concern due to its rapid onset and potentially severe consequences (JaSOn et al., 2018; Osman et al., 2020; Yuan et al., 2023). Unlike conventional droughts that develop over months or years, FD can manifest within weeks, leaving little time for preparation and mitigation (Pendergrass et al., 2020; Ford and Labosier, 2017). For example, a severe FD affected the central Great Plains and Midwest regions of the United States (US) in 2012, causing agricultural losses exceeding $30 billion (Otkin et al., 2019). The FD that occurred in 2017 resulted in agricultural losses of $2.6 billion in the Dakotas and Montana, U.S. (Dilling et al., 2019). FD occurs when precipitation (*P*) deficit is accompanied by above-average evaporative demand due to high temperatures, increased vapor pressure deficit, low humidity, and strong winds (Otkin et al., 2019, 2016). If such a condition persists for days to weeks, it will force the system to transition from an energy-limited state to a water-limited state, resulting in a rapid increase in soil moisture (SM) deficit and the development of FD in a region (Ford and Labosier, 2017; Hunt et al., 2014, 2009; Možný et al., 2012).

SM anomaly is a useful indicator for characterizing the onset of FD (Hunt et al., 2009; Možný et al., 2012). The rapid depletion of *SM* is one of the first signs of FD since evaporative demand directly contributes to *SM* depletion (Otkin et al., 2016; Ford and Labosier, 2017; Osman et al., 2020; Yuan et al., 2019). *SM* anomalies appear first in topsoil before moving deeper into the soil (Hunt et al., 2014; Ford et al., 2015). Decreased *SM* in the upper layer stimulates the vegetation roots to take up water from deeper soil depths (Baudena et al., 2013). Across the globe, significant advances have been made in exploring the changes of FD events at different *SM* layers (Shah et al., 2022; Zhang et al., 2022; Sungmin and Park, 2023) and in root zone soil moisture (RZSM) as a particular focus (Lesinger et al., 2022; Mahto and Mishra, 2023; Zheng et al., 2022). These valuable studies address multiple aspects of FD, including meteorological drivers, rate of intensification (*RI*), ecological impacts, and future assessment. However, the interaction between *SM* layers regarding FD vertical propagation has not been assessed before. It is unclear at what time lag FD events of the upper layer tend to propagate deeper soil layers in response to the meteorological anomalies. Evaluating the temporal dynamics of FD transmission across soil layers and related meteorological conditions enhances our understanding of drought mechanics, aiding local preparedness and response plans. In addition, there is no research focusing on the influence of *RI* on FD severity at various soil depths. It remains unknown whether the impacts of *RI* on drought severity are dependent on soil depth.

FD poses unique challenges for water resource management and agricultural planning, particularly in regions with high climate variability and strong land-atmosphere coupling (Basara et al., 2019a; Mahto and Mishra, 2020). The Indus Basin, spanning parts of Pakistan, India, China,

https://doi.org/10.5194/egusphere-2025-625
Preprint. Discussion started: 5 March 2025

and Afghanistan, is a transboundary basin with diverse climatic zones, ranging from arid lowlands to snow-capped mountains, supporting the livelihoods of over 268 million people (Laghari et al., 2012; Shafeeque et al., 2022). The water resources in this basin are already under stress due to population growth, agricultural intensification, and climate change (Immerzeel et al., 2016; Shafeeque et al., 2023; Shafeeque and Bibi, 2023), making it particularly vulnerable to rapid onset drought events. Despite the significant impacts of FD events, there is a notable gap in understanding the spatiotemporal dynamics and driving mechanisms of FD in the Indus Basin. Although several studies have investigated long-term drought patterns in the Indus Basin (Adnan et al., 2018; Ashraf et al., 2023; Ashraf et al., 2021; Abbas et al., 2021), research specifically focusing on FD remains limited. Aside from being studied in some valuable global-scale research (Neelam and Hain, 2024; Mahto and Mishra, 2023; Mukherjee et al., 2022; Sreeparvathy et al., 2022; Qing et al., 2022; Yuan et al., 2019; 2023), the in-depth investigation of FD characteristics in the Indus Basin is one of the crucial gaps in the literature. This gap is particularly concerning given the projected increases in climate variability and extreme events in this region (Lutz et al., 2016; Shafeeque and Bibi, 2023; Krishnan et al., 2019).

Here, based on the *SM* and meteorological data from the Global Land Data Assimilation System (GLDAS) over the period 1970-2023, this study presents a multi-layer FD evaluation method to explore the temporal evolution of FD from upper (0-10 cm) to middle (10-40 cm) and RZSM layer (100 cm) in the Indus Basin, a typical water-limited region, to improve our understanding of FD vertical propagation. Based on the timings of occurrences of FD events, we explore the simultaneous and subsequent FD events between different *SM* layers and compare the associated meteorological conditions to determine potential differences. Specifically, our study aims to address the following scientific questions: 1) how do the dynamics of FD vary across different soil depths in the Indus Basin, particularly regarding the spatio-temporal distribution of FD and the impact of *RI* on FD severity, 2) what is the tendency of the FD events to vertically propagate between different soil layers and the role of meteorological anomalies in the FD development? 3) what is the evolutionary behavior of meteorological variables before and after FD? and how do these variables influence *RI*?

This study contributes to the growing body of literature on FD by examining the vertical propagation of FD through the soil column, offering insights into their three-dimensional nature. Additionally, it provides valuable insights for improving drought monitoring, early warning systems, and water management strategies in the Indus Basin and similar complex river basins worldwide.

2 Methodology

2.1 Study area

The study domain covers the Indus Basin of South Asia, which is located at 22°–38°N and 65°–87°E (Fig. 1). The basin encompasses a total land area of 1.12 million km^2, shared by four adjacent countries namely Pakistan (47%), India (39%), China (8%), and Afghanistan (6%). It

https://doi.org/10.5194/egusphere-2025-625
Preprint. Discussion started: 5 March 2025

stretches from the western Himalayan-Karakoram-Hindu Kush Mountains in the north to the dry alluvial plains of Pakistan in the south. The Indus Basin has a unique climate, with a humid- semi humid climate in the north and a semi-arid to arid climate in the south (Hasson et al., 2019; Shamsudduha et al., 2019). The annual average precipitation in the basin is about 230 mm (Janjua et al., 2021), but the precipitation pattern is irregular, with pronounced variability in magnitude, time of occurrence, and aerial distribution (Ahmad et al., 2014). Temperature varies from below freezing (<0˚C) at higher elevations during winter to above 40˚C at lower elevations during summer (Krakuer et al., 2019). The mean annual potential evaporation ranges from 1650 to 2040 mm (Ali, 2013; FAO, 2011), and is expected to increase with global warming (Janjua et al., 2021).

In the past decades, this region has witnessed numerous severe and extreme drought events (1984–86, 1992, 1998–2002, 2007/08, 2012/13, 2017/18, and 2022) (Rahman et al., 2023), making it a critical area for study due to the significant drought impacts. For example, an extreme FD event occurred unexpectedly in late spring in 2022 and continued throughout the summer across Pakistan, with the temperature exceeding 51˚C in some parts of the country during May (Nanditha et al., 2023), leading to reduced wheat yield, livestock losses and health issues (Otto et al., 2022). This region is vulnerable to more frequent and intense drought events due to climate warming, which has significantly influenced food and water security (Ali et al., 2022).

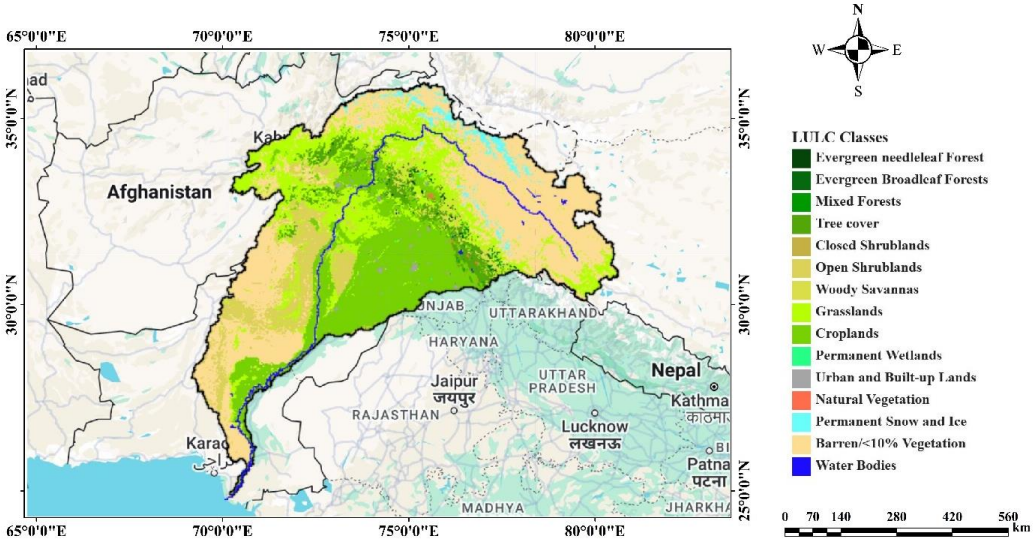

Figure 1. Study area map (Indus Basin) showing vegetation classes, derived from the MODIS dataset (https://code.earthengine.google.com/scriptPath/MODIS/061/MCD12Q1).

2.2 Data collection and processing

To quantify FD events and explore the associated meteorological driving mechanisms over the Indus Basin, the 8-daily data of *SM* at different depths (0-10 cm, 10-40 cm, 100 cm) and meteorological variables including precipitation (*P*), temperature (*T*), evapotranspiration (*ET*), and

https://doi.org/10.5194/egusphere-2025-625
Preprint. Discussion started: 5 March 2025

wind speed (*WS*) during 1970-2023 were collected from the GLDAS Version 2 (GLDAS-2) dataset with a horizontal resolution of 0.25˚ × 0.25˚. GLDAS-2 is reprocessed with the updated Princeton Global Meteorological Forcing Dataset (Sheffield et al., 2006) and upgraded Land Information System Version 7 (LIS-7). This dataset has been proven to effectively capture *SM* trends and patterns at both regional and global scales (Jia et al., 2018; Dorigo et al., 2012; Cheng et al., 2015). In this study, we construct an 8-daily average time series of all input variables to avoid high-frequency variability in hourly data.

2.3 Identification of FD at various soil depths

In this study, FD is defined based on *SM* at the 8-daily scale. We employ an 8-daily time scale, as it effectively captures temporal variations in hydrometeorological variables, and well reflects the rapid severity of FD as well as their impact on agroecosystem (Hu et al.,2025; Yang et al., 2023). We identify FD events at three different *SM* depths, i.e., 0-10 cm, 10-40 cm, and 100 cm, which directly affect the growth status of vegetation.

As *ET* is limited in winter, which prevents the rapid decline of *SM*, this study focuses on the growing season (April to October) and also includes the FD events that begin in March and end in April (Christian et al., 2020). An FD event occurs when the following conditions are met:

1. When the 8-daily mean *SM* (%) decreases from above the 40th percentile to the 20th percentile within 3-time steps (i.e., 24 days), it indicates the “onset” stage of FD. The 20th percentile of *SM* is selected as the drought threshold according to Yuan et al. (2019).
2. The average *RI* of *SM* is not less than 5% in the percentile during the onset of FD.

$$RImean = \frac{1}{n}\sum_{1=0}^{i}\left[\frac{SM(t_{i+1}) - SM(t_i)}{t_{i+1} - t_i}\right] \geq 5^{th}\,percentile \quad (1$$

3. After the onset phase, the average *SM* of the next three octads remains below 20%. The recovery stage of FD starts when the *SM* percentile begins to increase. Once the *SM* recovers to above the 20th percentile, the drought ends.

https://doi.org/10.5194/egusphere-2025-625
Preprint. Discussion started: 5 March 2025

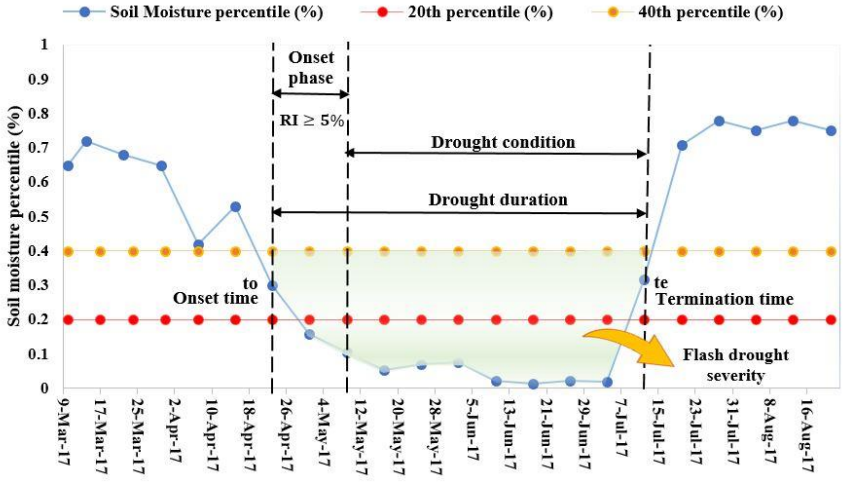

Figure 2. Illustration of the identification of FD.

Spatiotemporal characteristics of FD used in this study include the number of events, intensity, and severity. The severity refers to the accumulated *SM* percentile deficits from the 40% threshold (shaded area in Fig. 2) (Yuan et al., 2019). Intensity denotes the average *RI* during the drought onset period. The study period (1970-2023) is divided into two halves (1970-1996 and 1997-2023) to examine the evolutionary variations in FD characteristics over time.

We conduct the correlation analysis between *RI* and drought severity to explore the impacts of *SM* depth on FD characteristics at various soil depths.

In addition, we apply the one-way analysis of variance (ANOVA) to test the sensitivity of the impact of *RI* on drought severity to different *SM* layers. The ANOVA is a commonly used statistical hypothesis tool to evaluate the variations between two or more groups of observations (Hattermann et al., 2018). We constructed the null and alternate hypotheses as:

H_O = the impact of *RI* on drought severity is the same in all *SM* layers.

H_1 = the impact of *RI* on drought severity varies with respect to the depth.

The significance of any variations is determined by the *F-test* at the significance of 0.05. The *F-test* is recommended as a practical test, because of its robustness against many alternative distributions (Hattermann et al., 2018). The *F*-statistics explains the degree to which the variability in *RI* that can be attributed to the difference between soil layers is proportionately larger than the variability within each soil layer.

https://doi.org/10.5194/egusphere-2025-625
Preprint. Discussion started: 5 March 2025

2.4 Evaluation of Vertical propagation of FD events

The evolution of key meteorological factors (*P*, *T*, *ET*, *and WS*) directly affects the development of FD events. These driving factors can either confine the FD events to the upper layer or facilitate their penetration into deeper layers simultaneously or subsequently. In this study, we evaluate the vertical propagation of FD events between different layers (i.e., upper and middle) by comparing the two types of FD events: i) that occur in both layers at the same time ('*t*-events', i.e., simultaneous events), and ii) that occur in the middle layer at 1-lead time '*t*+1' time to the upper layer ('*t*+1 events', i.e., subsequent events). Further, meteorological anomalies are used to assess the difference in meteorological variations responsible for these two types of FD events. The monthly distributions of these FD events from March to October are also compared and evaluated to determine their probable timing of occurrence.

2.5 Analysis of driving forces of FD

The meteorological anomalies play an essential role in driving the development and recovery of FD events (Otkin et al., 2014). To understand the meteorological conditions associated with the FD occurrence, we evaluate the variability of *T*, *P*, *ET*, and *WS* anomalies before and during FD events at the 8-daily scale during the study period (1970-2023), which are calculated as follows:

$$Anomaly_t = \frac{x_y - \bar{x}}{\sigma} \quad (2$$

where 'x_y' is the actual 8-day average meteorological factor (*T*, *P*, *ET*, and *WS*) in '*t*' time steps for '*y*' year, '$\bar{x}$' is the mean 8-day average meteorological factor in '*t*' time steps for the study period, '$Anomaly_t$' is the anomaly in '*t*' time steps for '*y*' year.

The anomalies of *T*, *P*, *ET*, and *WS* are calculated for each grid cell across the study area. We evaluate their evolutionary behavior with two-time steps back (lag-2, lag-1) and forth (Lag+1, lag+2) and during the onset of FD events (lag0) using the boxplot distribution.

The multiple linear regression (MLR) model is further used to quantify the relative contribution of meteorological variables (*T*, *P*, *ET*, and *WS*) to *RI* (Ting et al., 2009; Cheng et al., 2015). The equation of MLR is expressed as follows:

$$RI_i = \alpha_0 + \alpha_1 X_{1i} + ... + \alpha_n X_{ni} \; (i = 1, 2, ..., m)$$

$$RI = \begin{bmatrix} RI_1 \\ RI_2 \\ . \\ . \\ RI_m \end{bmatrix}, \quad X = \begin{bmatrix} X_{11} & ... & X_{n1} \\ X_{12} & ... & X_{n2} \\ . & . & . \\ . & . & . \\ X_{1m} & ... & X_{nm} \end{bmatrix}, \quad \alpha = \begin{bmatrix} \alpha_0 \\ \alpha_1 \\ . \\ . \\ \alpha_n \end{bmatrix} \quad (3$$

https://doi.org/10.5194/egusphere-2025-625
Preprint. Discussion started: 5 March 2025

where $X_i = P_i$, T_i, ET_i, and WS_i are meteorological anomalies during the ith drought event; α_0 and $\alpha_{1\text{-}n}$ are intercept and regression coefficients, respectively; m indicates the number of events at a given grid cell; and RI_i represents the regressed rate of intensification at a given grid cell estimated by the MLR model. A regression coefficient reflects the importance of an independent variable to a dependent variable (Zhang et al., 2022). Using regression coefficients, we can determine the relative importance of meteorological variables on *RI*. The performance of the MLR model is evaluated based on the coefficient of determination (R^2):

(4

$$R^2 = \left(1 - \frac{\sum_{i=1}^{n}\left(RI_{obs}(i) - RI_{smi}\right)}{\sum_{i=1}^{n}\left(RI_{obs}(i) - \overline{RI_{obs}}\right)^2}\right)$$

where RI_{obs} (i) and RI_{smi}(i) are observed and simulated *RI* at the grid 'i', respectively; $\overline{RIobs}$ mean observed *RI*, n indicates the number of observations.

3. Results

3.1 FD characteristics at different SM layers

The maximum number of FD events during 1970-2023 is recorded in the upper layer (i.e., 44) demonstrated by the widespread spatial pattern of events across the basin (Fig. 3a), because it tends to respond quickly to atmospheric variability and interacts closely with the evaporative demand (Potkay et al., 2021; Jafari et al., 2021). However, we observe an obvious shift in the pattern of occurrence from the lower to middle basin during the first and second half of the study period (Figs. 3b & c). In the case of the middle layer, the number of FD events varies between 1-33 throughout the basin. The middle Indus basin experiences a maximum number of events (~ 21) between 1997 - 2023, which is revealed by the spatial extent from the east to the west and the southwestern region of the study area (Fig. 3f). Further, the analysis of RZSM shows that the increased spatial extent of events occurrences in the second half (1997-2023) is consistent with that of the other two layers, with the number of events ranging from 1 to 39. Generally, the middle basin located in the transition zone from humid to semi-humid and semi-arid is more prone to FD events.

https://doi.org/10.5194/egusphere-2025-625
Preprint. Discussion started: 5 March 2025

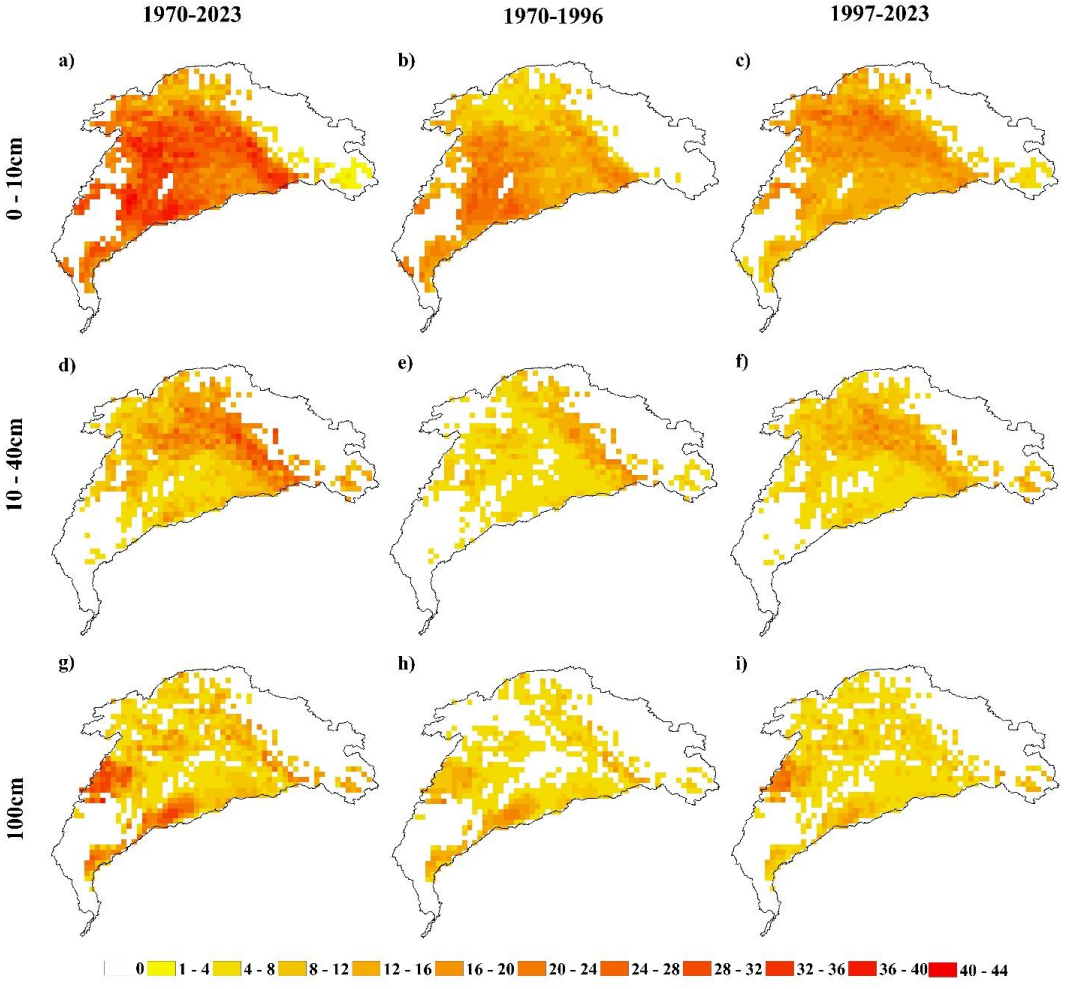

Figure 3. Spatial distributions of the number of FD events at three *SM* layers (0-10 cm, 10-40 cm, 100 cm) during the periods 1970-2023, 1970-1996, and 1997-2023.

Similarly, Figure 4 demonstrates the spatiotemporal pattern of the *RI* of the total FD events over the study period (1970-2023). The *RI* describes the average depletion rate of *SM* during the onset-development of FD (Xiang et al., 2020). According to Fig. 4, the spatial distribution of *RI* is consistent with the number of events at each layer. In general, a higher *RI* (i.e., 55 percentile) is observed in the middle basin, while a lower *RI* (i.e., < 5 percentile) is found in the southern part of the basin.

https://doi.org/10.5194/egusphere-2025-625
Preprint. Discussion started: 5 March 2025

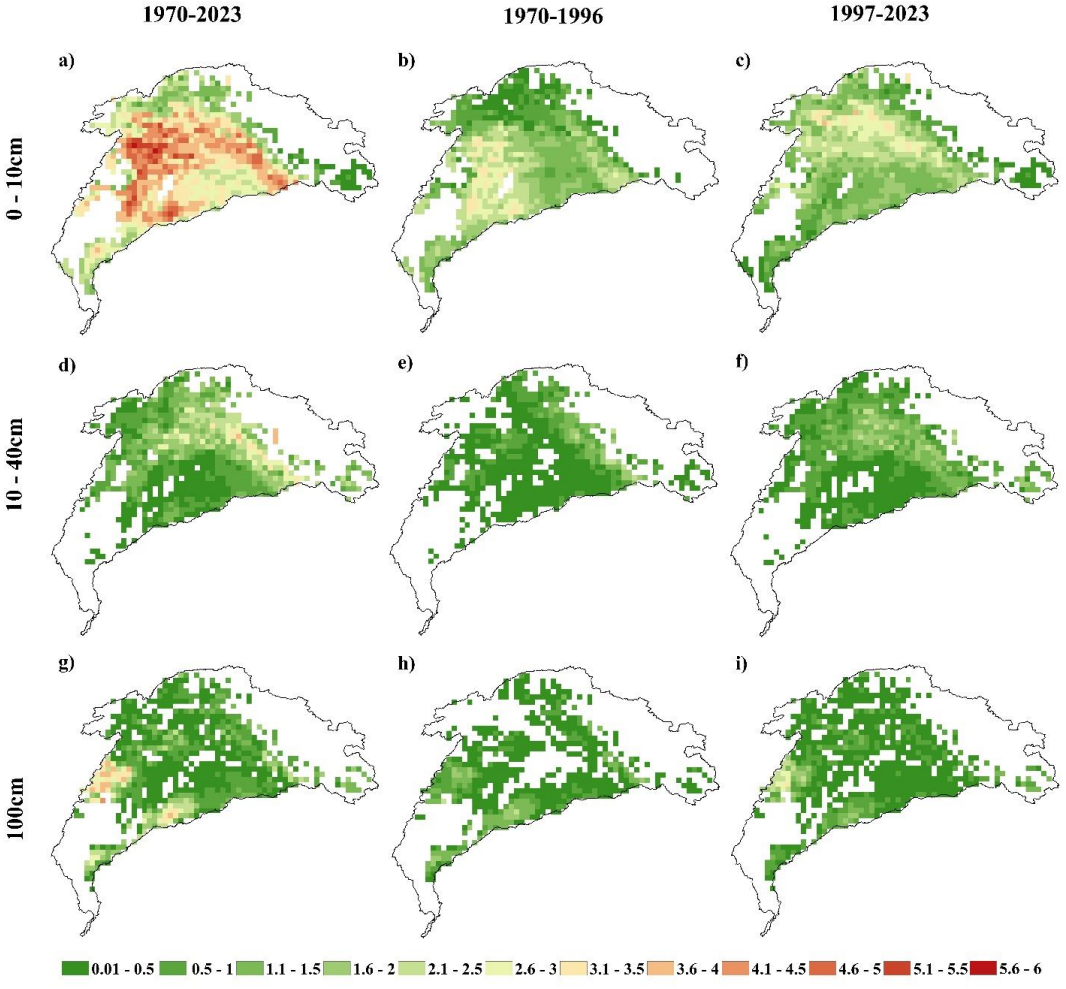

Figure 4. Spatial distributions of the average *RI* of the total FD events at three *SM* layers (0-10 cm, 10-40 cm, 100 cm) during the periods 1970-2023, 1970-1996 and 1997-2023

Fig. 5 shows the total accumulated severity of FD events over the Indus Basin during 1970-2023. In all three layers, the spatial pattern of severity is similar to the number of FD events at the grid scale. The middle Indus Basin experiences a higher severity than other regions. During 1997-23, we observe a noticeable variation in spatial extent. A significant rise in the number of events with higher severity is observed in the upper and the middle layers from the east to the west of the basin during 1997-2023 (see Fig. 5c & f). Similarly, the drought severity in the RZSM layer during 1997-2023 (Fig. 5i) is higher in the western region of the basin compared to 1970-1996 (Fig. 5h).

https://doi.org/10.5194/egusphere-2025-625
Preprint. Discussion started: 5 March 2025

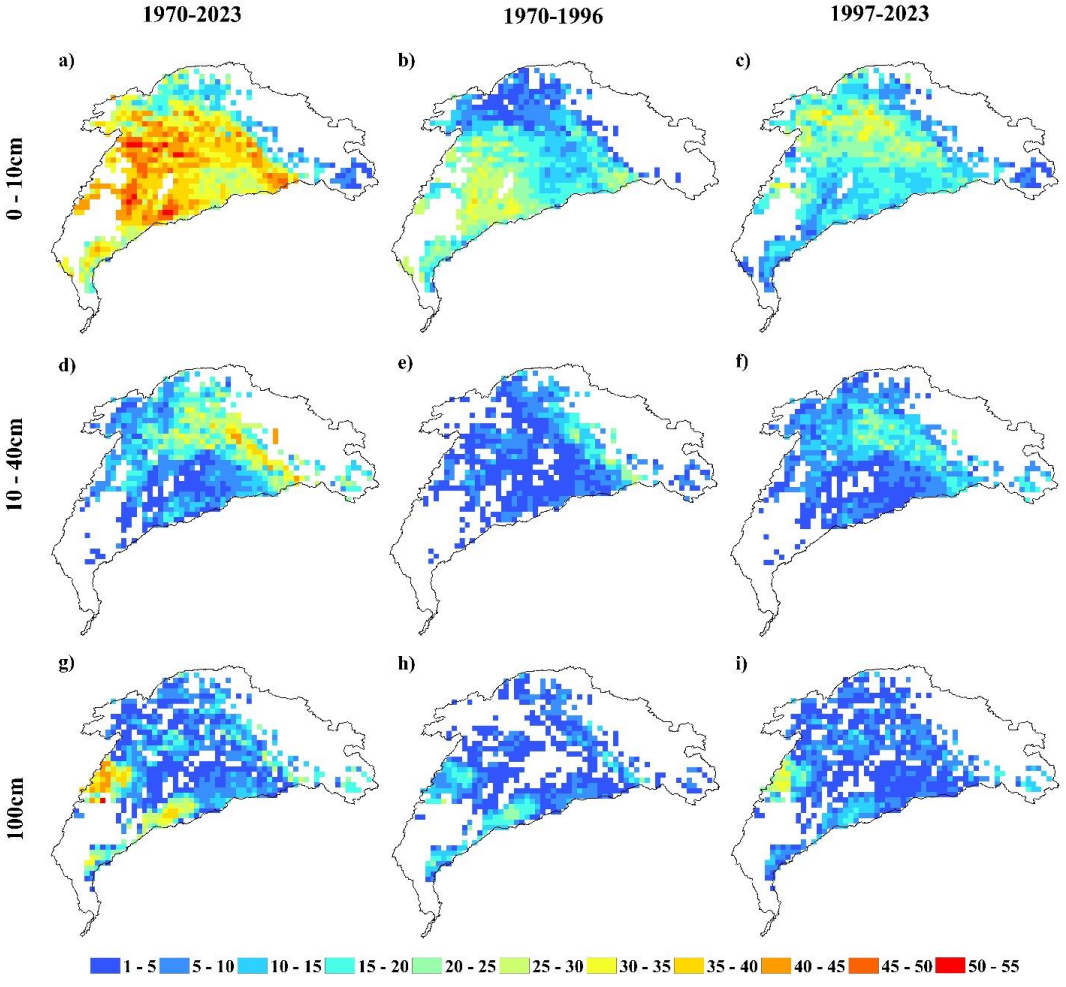

Figure 5. Spatial distributions of the total accumulated severity of FD events at three *SM* layers (0-10 cm, 10-40 cm, 100 cm) during the periods 1970-2023, 1970-1996 and 1997-2023

Fig. 6 demonstrates the spatial distributions of the correlation between *RI* and drought severity. In the upper layer, there is a weak correlation (r^2<0.35) between *RI* and severity over 94% of grids (Fig. 6a), suggesting that the *RI* shows little impact on drought severity in the upper layer. Comparatively, the middle layer exhibits a moderate to strong correlation (0.40 < r^2 <1.0) between *RI* and severity in some parts of the basin (Fig. 6b), especially in Punjab province (highlighted with a red circle, r^2>0.9), which is covered by flat alluvial land and has extensive agricultural activities (Abbas et al., 2013; Kumar et al., 2013). Similarly, a strong correlation is found in RZSM (Fig. 6c), with the r^2 ranging from 0.4 to 1 across the middle Indus Basin, especially in Punjab province (encircled with red color). This may be due to the fact that the vegetation facilitates

https://doi.org/10.5194/egusphere-2025-625
Preprint. Discussion started: 5 March 2025

drawing more water from deep soil during the drought condition to fulfill the evaporative demand (Wang et al., 2016). Moreover, the strength of the correlation can be attributed to the persistency of *SM* at different soil depths, which is supported by the analysis of ANOVA, showing that the difference between the layers is statistically significant (F =18.0193, p<0.05). It is noteworthy that there is a weak correlation (r^2 <0.2) in the south-western part of the basin (blue dotted area) (Fig. 6c), where more frequent FD events are detected (see Fig. 3g). It can be attributed to the low moisture content in this part of the basin, which leads to a weak response to high evaporative demand, resulting in a poor correlation between *RI* and FD severity. Hence, the above analyses suggest that the middle Indus Basin exhibits a significant influence of *RI* on severity. Moreover, the spatial heterogeneity of *SM* influences drought severity.

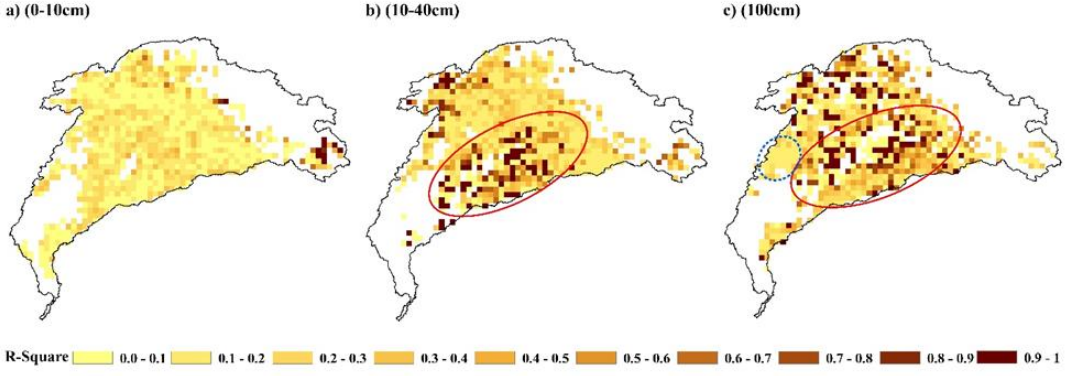

Figure 6. Spatial distributions of the correlation coefficients (r^2) between *RI* and drought severity for each *SM* layer.

3.2 Vertical propagation of FD events across the SM layers

We identify 2148 '*t*-events' and 1154 '*t*+1 events' during 1970-2023 (see Fig. 7e). Both types of events are spatially distributed across the middle Indus Basin and some parts of the upper Indus Basin (Figs. 7a & c), where overall climate varies from humid to semi-humid, supporting vegetation growth and agricultural activities. However, the spatial extent of the '*t*-events' is greater than the '*t*+1 event'. As '*t*-events' are characterized by the immediate and severe *SM* deficits from the upper to the middle *SM* layer that can cause severe risk to the ecosystem. While, in the case of the '*t*+1 event', when the decline in *SM* in the middle layer occurs at the one-time step after the decrease in the upper layer, it suggests a slightly slower progression of dryness from the upper to deeper layer. These events can exacerbate the drought impacts initiated by the upper layer, as the prolonged dry conditions in the middle layer can lead to extended periods of drought stress for vegetation. This transferring impression of FD from the upper to the deeper layer is in line with the existing literature, which indicated that with the development of FD, the *SM* deficit first appears in the upper moisture layer, and then leads to further downward movement of the deficit to the deeper layers (Otkin et al., 2016; Anderson et al., 2013). The finding of the vertical FD propagation highlights the importance of *SM* monitoring at various depths in drought monitoring systems.

https://doi.org/10.5194/egusphere-2025-625
Preprint. Discussion started: 5 March 2025

Figs 7b & d explain the monthly distribution of FD events between March to October. September witnessed the maximum number of both types of events throughout the study period (1970-2023) followed by April for '*t*-events', and May for '*t*+1 events'. Moreover, for the '*t*+1 events', the number of events gradually increases from March to May (Fig. 7d), indicating an increased likelihood of the FD occurrence from spring to early summer. The emergence of '*t*-events' and '*t*+1 events' during these months are in line with the FD event that occurred in the US Northern High Plains in 2017, where warm-dry weather during spring and early summer caused a severe drought over two months (Otkin et al., 2019). Similarly, a large number of FD events in Spain were recorded during spring and summer (Noguera et al., 2020).

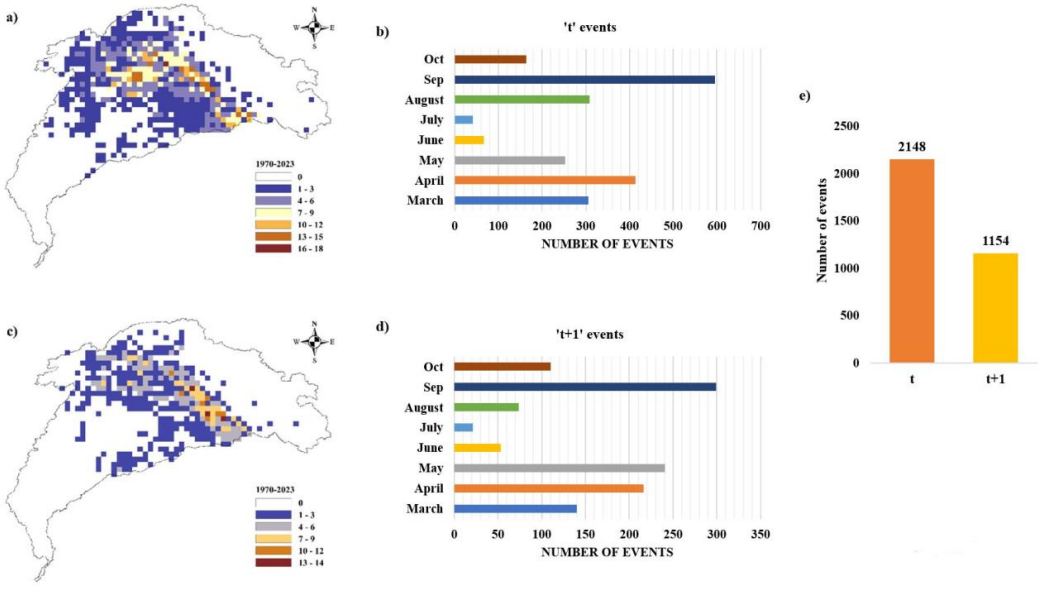

Figure 7. Vertical propagation of FD events between different *SM* layers. (a) shows the events in both layers at the same time '*t*', and (c) events in the deep layer at 1 lead time '*t*+1' time with respect to the upper layer. b) and d) explain the monthly distribution of '*t*' and '*t*+1' events, respectively. e) shows the total number of '*t*' and '*t*+1' events.

3.3 Meteorological driving mechanism of FD

Based on the correlation results in 4.1 section, we use the RZSM to assess the meteorological evolutionary behavior associated with FD events. Fig. 8 illustrates the boxplot distribution of the anomalies of four meteorological variables before and after the FD events at each time step (lag-2 to lag+2). The higher maximum *T* anomalies are > 2 standard deviations (STDs). The distribution pattern for each time step (lag-2 to lag+2) shows that the median of *T* anomalies is lower at lag-1, but becomes stronger at the onset (lag0) and after the onset of FD (Fig. 8a).

https://doi.org/10.5194/egusphere-2025-625
Preprint. Discussion started: 5 March 2025

Unlike *T* anomalies, the median of *P* anomalies shows a decreasing trend among all temporal lags (i.e., lag-2 to lag+2, Fig. 8b), with the maximum negative anomaly of -1.5 STDs. There is an obvious decrease in maximum positive *P* anomalies from lag-2 to lag-1, indicating the development of conditions leading to drought occurrence. From lag-1 to lag+2, the maximum *P* anomalies tend to show a negative STD (i.e., > -1 STD), with the median around -0.5 STD. Overall, the *P* anomalies remain negative before and during the onset of FD events, and this behavior persists as drought progresses. It is important to note that significant negative *P* anomalies may result in an increase in *T* that rapidly dries out *SM*. The depletion of *SM* due to the negative *P* anomalies could lead to a decrease in *ET*, leading to higher *T* and vapor pressure deficits (VPDs). A higher VPD further accelerates the *SM* depletion (Zhou et al., 2019). Moreover, the negative *P* anomalies accompanied by the positive *T* anomalies can intensify the atmospheric water demand, thus further speeding up *SM* decline and triggering FD in a region (Mahto and Mishra, 2020).

The distribution pattern of *ET* anomalies shows a shift from negative (lag-2) to positive anomalies (lag-1 and lag0) (Fig. 8c), which coincides with positive *T* and negative *P* anomalies during lag-1 and lag0 (see Figs. 8a & b). The median of *ET* anomalies becomes more negative (> -2 STD) as the drought proceeds (from lag+1 to lag+2), which indicates the worsening of the drought condition. In this situation, the high *T* increases evaporative demand, leading to a system from energy-limited to water-limited states. The distribution pattern of *WS* does not reveal the distinguished variations before and after FD (Fig. 8d). The higher maximum positive *WS* is observed at lag0 (> 3 STDs), while the median remains positive and slightly tends to increase from lag-1 to lag+2. All in all, the variations in the behavior of *T*, *P*, *ET*, and *WS* during different stages of FD indicate a close association between FD development and meteorological variabilities in this region, which is consistent with the previous findings (Mo et al., 2016; Yuan et al., 2019).

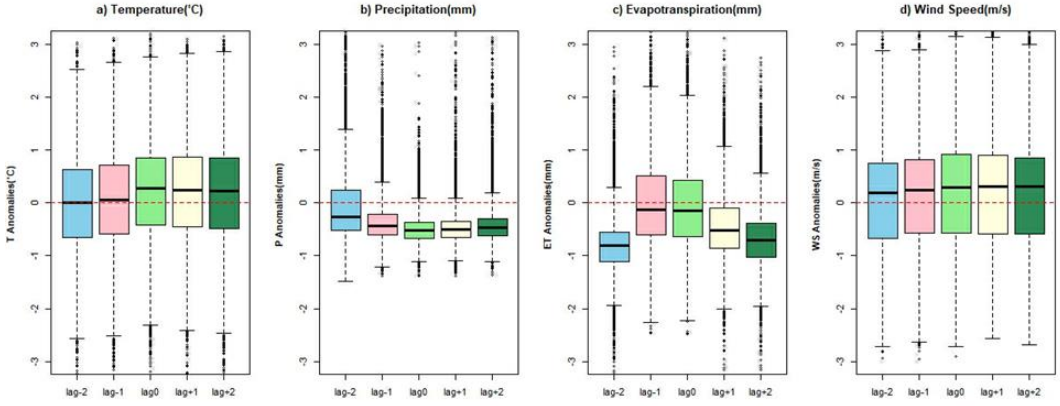

Figure 8. Boxplots of the standardized anomaly values of meteorological variables in adjacent time steps of FD events at the RZSM layer (100cm) during 1970-2023 extracted from all grids over the Indus Basin. Lag-2, and lag-1 show time steps prior to the FD onset, lag0 represents FD onset time, and lag+1 and lag+2 show the time steps after the onset of FD.

https://doi.org/10.5194/egusphere-2025-625
Preprint. Discussion started: 5 March 2025

Further, to examine meteorological variabilities associated with the '*t*' and '*t*+1' FD events, we used a common factor anomalies approach mentioned above. Regarding the meteorological variabilities associated with '*t*-events', we observe an increase in the median of *T* from lag-1 to lag+2 (Fig. 9i(a)), with the highest positive *T* deviation at lag+1. In the case of *P*, the median decreases from lag-1 to lag+1, and the maximum *P* deficit continues until lag+2 (Fig. 9i(b)). This coevolution ultimately reduces the humidity level of the system, which appears from the *ET* variability from lag0 to lag+2 (Fig. 9i(c)). However, for *WS*, there is a slight increase in median from lag0 to lag+1, suggesting an increase in positive anomalies after the onset of FD.

Compared with '*t*-events', we observe drastic *P* deficits and high *T* at lag-1 for '*t*+1 events' (Fig. 9ii (a & b)). These FD events evolve from the events that appeared at the upper layer, hence inheriting the particular impression of meteorological variabilities that can sustain drought characteristics. The maximum *T* anomalies are > 2.5 STDs from lag-1 to lag+2, with the positive median during this time frame (Fig. 9ii(a)). We notice persistent negative *P* anomalies from lag-1 to lag+1 (Fig. 9ii(b)), with the values slightly increasing from lag+1 to lag+2 but still below 0. On the other hand, the median of *ET* anomalies gradually decreases from lag-2 to lag+2 (Fig. 9ii(c)), which coincides with the variability of *T* and *P* (Fig. 9ii (a & b)). The increase in *T* and decrease in *P* from lag-2 to lag+2 substantially decrease *SM*, thereby reducing *ET*.

https://doi.org/10.5194/egusphere-2025-625
Preprint. Discussion started: 5 March 2025

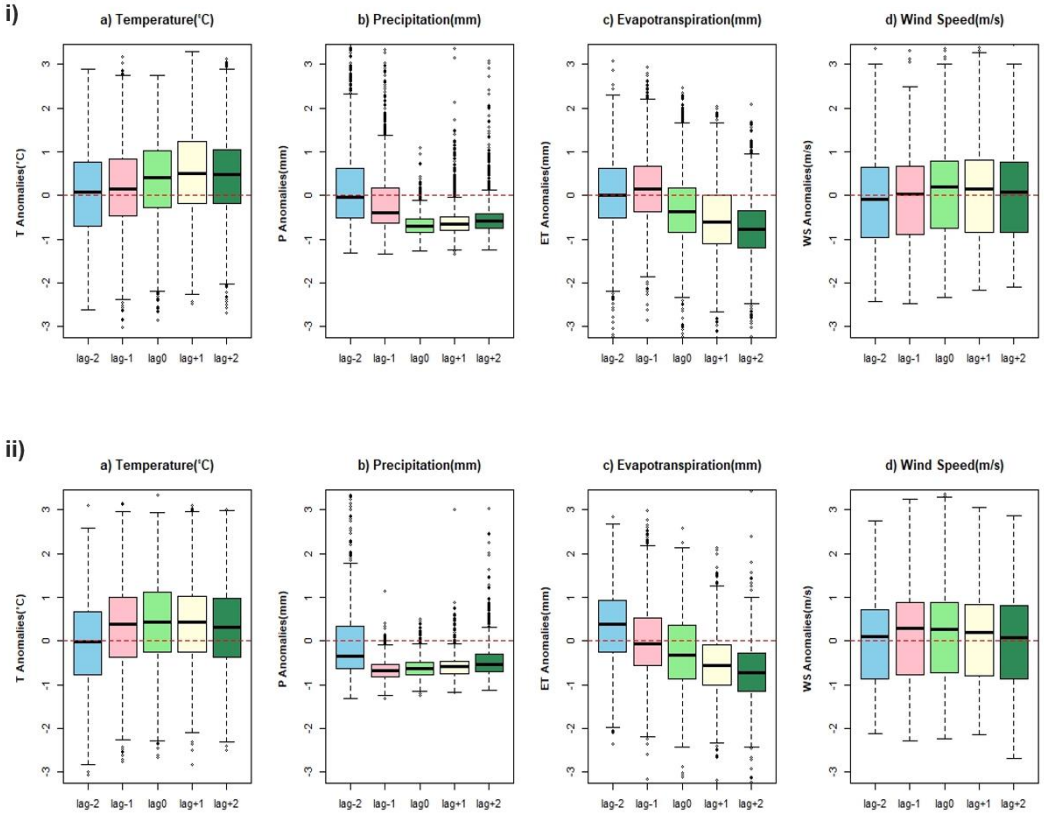

Figure 9. Same as in Figure 8, but for (i) '*t*-events' and (ii) '*t*+1 events'.

Figure 10a demonstrates the weights of meteorological anomalies contributing to *RI* during the onset development phase of FD events. On average, we observe the largest negative weight of *P* anomalies, suggesting the dominant role of *P* deficit in the FD onset in this domain. *T* and *ET* present nearly equal contributions to *RI*, which is in line with Koster et al. (2019), stated that the *P* deficit is the main driver of the FD occurrence. The model demonstrates a strong coefficient of determination (R^2 > 0.9) in the middle Indus Basin (see Fig. 10b), suggesting a significant contribution of meteorological variables to *RI*. In contrast, a weak R^2 (~ 0.4) is found in the southern region of the basin. Overall, the spatial pattern of R^2 is in harmony with the findings in Fig. 6, suggesting that the middle Indus Basin is more sensitive to FD occurrence compared to other regions.

https://doi.org/10.5194/egusphere-2025-625
Preprint. Discussion started: 5 March 2025

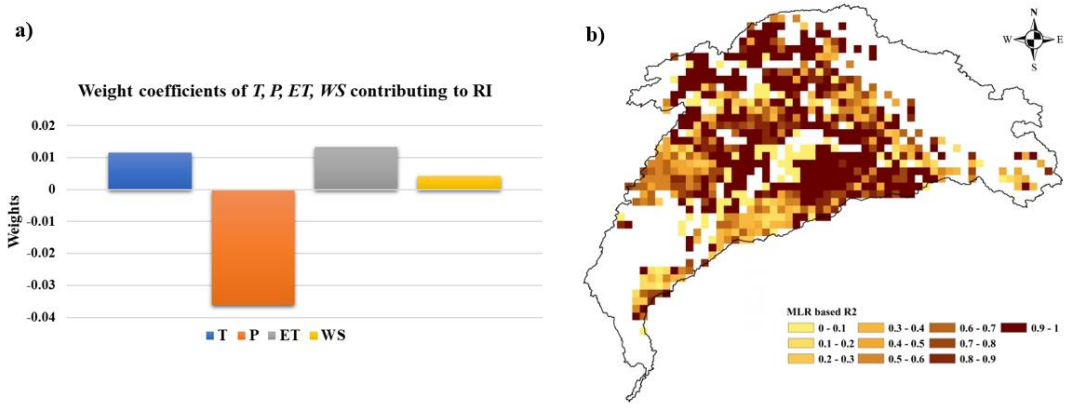

Figure 10. a) Weight coefficients of meteorological variables (*T, P, ET, WS*) contributing to *RI* during the development phase of FD. b) Spatial distribution of the coefficient of determination (R^2) of the model fitted by the multiple linear regression (MLR).

4. Discussions

4.1 Impact of SM dynamics on FD characteristics

This study finds the occurrence of FD events at each *SM* layer. However, the FD frequency is much larger in the upper layer compared to the deeper layer, mainly because the *SM* within the upper layer is most sensitive to meteorological variability, allowing more events to be detected. The results are consistent with a previous study on California (Cheng et al., 2016), which reported a higher drought frequency within the upper *SM* layer. We observe a distinctive increase in the spatial extent of FD events in the second half (1997-2023) of the study period (Figs. 3c, f, and i). It is important to discuss here that anthropogenic-driven climate warming has changed considerably around 2000 (Zeng et al., 2023). Recent studies have shown a dramatic increase in atmospheric water demand since 2000, leading to more frequent occurrence of heatwaves and other related disturbances including *P* and *SM* deficits (Williams et al., 2020; Perkins-Kirkpatrick et al., 2020). Our findings are in good agreement with Ullah et al. (2024), reporting the intensification in FD frequency and severity in Sri Lanka, Afghanistan, Pakistan, and India during 2010-2020. Moreover, the results highlight the tendency of the humid and semi-humid regions to induce FD, which has also been appreciated in previous research (Basara et al., 2019b). During 1997-2023, the number of FD events is noticeably amplified in humid and semi-humid regions of the middle Indus Basin, which leads to a higher variability in *SM* dynamics and results in more frequent drier and wetter anomalous conditions in such regions. Shah et al. (2022) reported a high occurrence of FD in humid regions. Chen et al. (2021) also reported a higher possibility of the FD occurrence in regions that have higher *SM* variability.

There are various vegetation types (crops, grassland, and forests) in the middle Indus basin due to the humid to semi-humid climate (Fig. 1). Such regions are likely to sustain *ET* in response to higher *T* as long as vegetation roots make water available from the system to fulfill the evaporative demand (Christian et al., 2019b; Zhu et al., 2021), hence developing the favorable

https://doi.org/10.5194/egusphere-2025-625
Preprint. Discussion started: 5 March 2025

conditions for the FD occurrence. This is in accordance with Guo et al. (2023), which demonstrated the role of vegetation water consumption in the onset of FD in humid regions. Zeng et al. (2023) also reported an increase in FD frequency in humid regions of the Amazon basin and Congo basin. Similar findings were noted in Russia where FD occurred in agricultural areas including Central, Volga, and southern federal districts of southwestern Russia in 2010 due to *P* deficit (Christian et al., 2020). In contrast in arid regions, higher *T* inhibits *ET* due to the limited *SM* availability (Mo et al., 2016; Yuan et al., 2019), resulting in a lower likelihood of FD occurrence than in humid regions (Wang et al., 2016).

The relationship between *RI* and drought severity is very sensitive to the spatial and vertical variability in *SM*, and a stronger correlation ($r^2 > 0.7$) is found in the middle and RZSM layers compared to the upper layer. This indicates that the impact of *RI* on drought severity varies with soil depth. This variability across the vertical *SM* column apprehends a more holistic dynamics of *SM* variation (Berg et al., 2017). Also, regarding the spatial extent, the correlation between *RI* and drought severity is stronger in the regions with higher *SM* level. Consequently, moisture from the system is depleted considerably in response to the higher *RI*.

As significant agriculture activities are carried out in the middle Indus Basin, the occurrence of FD events can pose substantial impacts on vegetation productivity. Hence, it is evident that the frequency of FD events alone does not dictate the severity of drought impacts on the system. The other factors, such as *SM* deficit at different depths, *RI*, and land characteristics also play critical roles in exacerbating drought severity. In conclusion, we can say the FD events that occurred in the middle and RZSM layers can produce significant impacts on agroecosystem and water resources, and the varying effects of *RI* at various soil moisture layers can pose a potential concern for different types of vegetation.

4.2 Influence of land-atmosphere interaction on the FD vertical propagation

The soil water content in the vertical soil profile plays an important role in the soil-plant-atmosphere continuum system (Western et al., 2004). The assessment of the vertical propagation of FD events between different *SM* layers shows that the middle Indus Basin and some lower parts of the upper Indus Basin are more susceptible to FD. Given the combined effect of *P* deficit and high *T* (Figs. 9i & ii), the amount of *ET* could increase in a short period ultimately leading to the development of simultaneous '*t*' and subsequent '*t*+1' FD events. The increase in transpiration during the growing season exacerbates the rapid decline in *SM* (Koirala et al., 2017). According to Qing et al. (2023), the increasing drying trend of soil water in humid regions corresponds to positive *T* and negative *P* anomalies. This deficit of moisture within the surface, sub-surface soil, and atmosphere ultimately results in a drier vertical atmosphere over a region (Dimri et al., 2019). However, this pattern cannot be acquired in arid regions, because sparse or no vegetation reduces *ET* due to limited *SM* supply (Qing et al., 2022; Gupta et al., 2020).

This is the first study investigating the temporal relationship in FD occurrence across different *SM* layers. The analysis of the '*t*+1' events reveals that the relationship between different

https://doi.org/10.5194/egusphere-2025-625
Preprint. Discussion started: 5 March 2025

SM layers is influenced by variations in the moisture content of the upper *SM* layer, which facilitates the vertical propagation of FD. The temporal differences in the occurrence of '*t*+1' FD events can be associated with the persistence of certain meteorological conditions in a region that drive the vertical depletion of *SM* over time (Fig. 9ii). Moreover, the loss of moisture from different soil depths is affected by different factors. For example, soil evaporation and transpiration mainly consume the water in the upper soil layer, whereas water loss in the deeper soil layers depends on transpiration, which leads to different responses to meteorological anomalies at various time lags.

On the other hand, the '*t*' events result from the simultaneous depletion of *SM* from the upper layer to the deeper layer, indicating the rapid development of FD conditions due to deeper moisture loss, and reflecting the dynamic behavior of the FD phenomenon over the same region. Overall, the study provides new insights into how the varying moisture conditions at different soil depths affect the occurrence and dynamics of FD events that can be important for FD monitoring and prediction systems for a region.

The results also indicated that the *'t'* and *'t+1'* events occur most frequently in spring and early summer (Figs. 7b & d). During this season, a dipolar system develops over southern Asia expanding from east to west, which actively propagates the pressure gradient and adiabatic wind, greater condensation, and *P* deficit, thereby amplifying the FD occurrence in this region (Ullah et al., 2024). Moreover, vegetation growth can also affect the development of FD. As warming *T* advances the spring leaves' emergence (Fu et al., 2015), the plant growth in the early stages may reduce *SM* in late spring due to enhanced *ET* (Angert et al., 2005; Peñuelas et al., 2001). The *SM* deficits may continue till summer due to further increased *T* and lead to more severe FD. This may explain the occurrence of FD in vegetative-dominant areas, particularly during spring and summer (Figs. 7a & c). The spatial extent of these extreme FD events is relatively less compared to the total extent of all FD events recorded in each *SM* layer (Fig. 3). Xu et al. (2021) also found that the areas affected by extreme drought decrease with the increase of soil depth during the most severe stage of drought. This may be related to the differences in the persistency property of *SM* at different depths.

4.3 Contribution of meteorological anomalies to the FD occurrence

The rapid onset of FD is attributed to local moisture imbalance caused by anomalies in *P* and *T*. The simultaneous occurrence of meteorological anomalies may cause rapid development of FD by decreasing *SM* (Basara et al., 2019b; Burrows et al., 2019; Fischer et al., 2007; Soares et al., 2019; Qing et al., 2022). We analyzed the variations in meteorological variables (*T*, *P*, *ET*, and *WS*) at different lags (lag-2 to lag+2) before and after FD to explore the underlying mechanism of FD development. We observe negative *P* and *ET* anomalies and positive *T* anomalies during the FD onset phase (Fig. 8). The negative *ET* anomalies correspond to the low *SM* during FD (Osman et al., 2020). The consistent *P* deficits can cause a decrease in *ET* leading to a higher *T* and vapor pressure deficit, which contributes to the onsets of heatwave and *SM* deficiency. This type of FD is considered a precipitation deficit FD (Zhou et al., 2019). The decrease in *ET* is also the result of rising *T* in a region (Zhang et al., 2017). The FD in Russia developed in July and mid-August in

https://doi.org/10.5194/egusphere-2025-625
Preprint. Discussion started: 5 March 2025

2010 due to *P* deficit and previously desiccated land surface, and led to a rapid rise in surface *T* and vapor pressure deficit. Christian et al. (2020) suggested the impact of FD as a potential precursor to heatwaves.

Fig. 8 shows that the meteorological anomalies persist as the drought proceeds, which suggests that the Indus Basin is more prone to precipitation deficit FD. Similarly, the occurrence of FD in the neighboring country of India during the monsoon season may be associated with the delay or reduction in monsoon rainfall (Christian et al., 2020; Mahto and Mishra, 2020). However, *WS* anomalies do not show obvious variations before and after the FD occurrence (Fig.8 & 9), which is consistent with the existing studies (Liu et al., 2020; Gou et al., 2021; Li et al., 2022) reporting no significant positive or negative *WS* anomalies during FD.

We also investigate the impacts of meteorological variables on *RI*, which is an important characteristic that distinguishes FD from conventional drought (Otkin et al., 2019). The meteorological forcing of FD is stronger than that of conventional drought (Ford and Labosier, 2017), which explains the close interaction between *RI* and meteorological conditions. The MLR analysis highlights the dominant role of *P* in influencing *RI*, followed closely by *ET* and *T*. The model demonstrates a strong coefficient of determination ($R^2 > 0.9$) in the middle Indus Basin and semiarid region of Punjab province, which is sensitive to the interaction of land and atmosphere. For example, a decrease in *SM* can lead to a decrease in *ET* and limit the local sources of boundary layer moisture, ultimately reducing atmospheric moisture advection. Subsequently, the atmosphere remains dry, increasing evaporation demand, and the dry soil is not conducive to convective rainfall, thereby exacerbating FD (Basara et al., 2019a, 2019b; Christian et al., 2019).

Overall, our study highlights the importance of the early warning systems being reconstructed to incorporate the FD phenomenon based on the understanding of the mechanism involved in FD development. FD is more likely to develop in humid and sub-humid regions, with more severe impacts on ecosystems and agriculture. Therefore, developing a framework involving improvement in the early warning system, preparedness, and modification in existing strategies can help prepare a proactive system and minimize the expected losses.

5. Conclusion

This study provides the first comprehensive analysis of FD dynamics in the Indus Basin, revealing complex spatiotemporal patterns and vertical propagation characteristics. The results indicate a higher occurrence of FD events in the middle Indus Basin in 1997-2023 compared to 1970-1996, suggesting an increased risk of FD over time in this region. The FD events are more prone to occur in the humid and sub-humid regions of the middle Indus Basin. Their frequency tends to decrease from the upper to the RZSM layer, with the strongest correlation between *RI* and severity ($r^2 > 0.9$) in the middle and RZSM layers, which is linked to the persistency of *SM*.

The vertical propagation analysis suggests that the susceptibility of the region to FD is driven by rapid loss of deeper *SM* ('*t*') and slower depletion of *SM* from upper to deep soil ('*t*+1'). Moreover, the number of '*t*' events and their spatial extent are greater than that of '*t*+1' events.

https://doi.org/10.5194/egusphere-2025-625
Preprint. Discussion started: 5 March 2025

There is a close relationship between meteorological conditions (rapid *T* rise and *P* decline) and FD development, especially in the '*t*+1 events' at lag-1. The temporal differences in the '*t*+1' FD events are closely related to the persistence of meteorological conditions. In contrast, the '*t*' events are caused by the simultaneous depletion of *SM* from the upper layer to the deeper layer. The MLR analysis further suggests that *P* is the most contributing factor affecting *RI*, followed closely by *T*.

These findings have significant implications for drought management and early warning systems in the Indus Basin, informing more effective agricultural and water management practices. Future research will focus on the transition from FD to conventional drought, investigating the impacts of climate and land cover changes, and developing coupled land-atmosphere models to improve FD prediction.

Appendix A: List of abbreviations used in this study

FD	Flash Drought
SM	Soil Moisture
RZSM	Root zone soil moisture
RI	Rate of Intensification
T	Temperature
P	Precipitation
ET	Evapotranspiration
WS	Wind speed
MLR	Multiple linear regression

Data Availability

The dataset used in this research is publicly available at Google Earth Engine and can be accessed from the following link: http://earthengine.google.com/.

Author Contribution

Tahira Khurshid developed the methodology, conceptualization, data collection, performed the analysis, writing and original draft preparation, Qiongfang Li supervision, funding acquisition, review and editing, Chuanhao Wu funding acquisition, review, editing and refinement of draft, Akif Rahim supported for data acquisition and FD identification, Muhammad Shafeeque Writing, review and editing, Shanshui Yuan, Zia Ul Hassan, Junliang Jin review and editing.

https://doi.org/10.5194/egusphere-2025-625
Preprint. Discussion started: 5 March 2025

Competing interests

The authors declare that they have no conflict of interest.

Financial Support

This work is supported by the National Natural Science Foundation Commission of China (Grant number 524034911).

References

Abbas, F.: Analysis of a Historical (1981–2010) Temperature Record of the Punjab Province of Pakistan, Earth Interact, 17, 1–23, https://doi.org/10.1175/2013ei000528, 2013.

Abbas, S., Kousar, S.: Spatial analysis of drought severity and magnitude using the standardized precipitation index and streamflow drought index over the Upper Indus Basin, Pakistan, Environ. Dev. Sustain, 23, 1–27, https://doi.org/10.1007/s10668-021-01299-y, 2021.

Adnan, S., Ullah, K., Shuanglin, L., Gao, S., Shouting Gao, Khan, A.H., Skov, H., Rashed Mahmood, Mahmood, R.: Comparison of various drought indices to monitor drought status in Pakistan, Clim. Dyn, 51, 1885–1899, https://doi.org/10.1007/s00382-017-3987-0, 2018.

Ahmed, K., Kamal, A., Shahid, S., Chung, E.-S., Wang, X., Harun, S.: Climate change uncertainties in seasonal drought severity-area-frequency curves: Case of arid region of Pakistan, J. Hydrol, 570, 473–485, https://doi.org/10.1016/j.jhydrol.2019.01.019, 2019.

Ahmad, S., Hussain, Z., Qureshi, A.S., Majeed, R., Saleem, M.: Drought mitigation in Pakistan: current status and options for future strategies, Colombo, Sri Lanka, International Water Management Institute, Vol. 85, ISBN 92-9090-580-8, 2004.

Ahmad, W., Fatima, A., Awan, U.K., Anwar, A.A.: Analysis of long term meteorological trends in the middle and lower Indus Basin of Pakistan—A non-parametric statistical approach, Glob. Planet. Change, 122, 282–291, https://doi.org/10.1016/j.gloplacha.2014.09.007, 2014.

Ali, A.: Indus Basin floods: Mechanisms, impacts, and management, Asian Development Bank, Mandaluyong City, Philippines, ISBN 978-92-9254-284-9, 2013.

Ali, S., Liu, D., Fu, Q., Cheema, M.J.M., Pal, S.C., Arshad, A., Pham, Q.B., Zhang, L.: Constructing high-resolution groundwater drought at spatio-temporal scale using GRACE satellite data based on machine learning in the Indus Basin, J. Hydrol, 612, 128295–128295, https://doi.org/10.1016/j.jhydrol.2022.128295, 2022.

Anderson, M.C., Hain, C., Otkin, J.A., Zhan, X., Mo, K.C., Svoboda, M., Wardlow, B.D., Pimstein, A.: An Intercomparison of Drought Indicators Based on Thermal Remote Sensing and

https://doi.org/10.5194/egusphere-2025-625
Preprint. Discussion started: 5 March 2025

NLDAS-2 Simulations with U.S. Drought Monitor Classifications, J. Hydrometeorol, 14, 1035–1056. https://doi.org/10.1175/jhm-d-12-0140.1, 2013.

Angert, A., S. Bonfils, C., Henning, C.C., Buermann, W., Pinzon, J.E., Tucker, C.J., Fung, I.: Drier summers cancel out the CO2 uptake enhancement induced by warmer springs, Proc. Natl. Acad. Sci. U. S. A, 102, 10823–10827, https://doi.org/10.1073/pnas.0501647102, 2005.

Ashraf, M.S., Shahid, M., Waseem, M., Azam, M., Rahman, K.U.: Assessment of Variability in Hydrological Droughts Using the Improved Innovative Trend Analysis Method, Sustainability, 15, 9065–9065, https://doi.org/10.3390/su15119065, 2023.

Ashraf, S., Nazemi, A., AghaKouchak, A.: Anthropogenic drought dominates groundwater depletion in Iran, Sci. Rep, 11, 9135–9135, https://doi.org/10.1038/s41598-021-88522-y, 2021.

Basara, J.B., Christian, J.I., Wakefield, R.A., Otkin, J.A., Hunt, E.H., Brown, D.P.: The evolution, propagation, and spread of flash drought in the Central United States during 2012, Environ. Res. Lett, 14, 084025, https://doi.org/10.1088/1748-9326/ab2cc0, 2019a.

Basara, J.B., Otkin, J.A., Hunt, E.D., Wakefield, R.A., Flanagan, P.X., Xiao, X.: A Methodology for Flash Drought Identification: Application of Flash Drought Frequency across the United States, J. Hydrometeorol, 20, 833–846, https://doi.org/10.1175/jhm-d-18-0198.1, 2019b.

Baudena, M., Hardenberg, J.V., Provenzale, A.: Vegetation patterns and soil-atmosphere water fluxes in drylands, Adv. Water Resour, 53, 131–138, https://doi.org/10.1016/j.advwatres.2012.10.013, 2013.

Berg, A., Sheffield, J., Milly, P.C.D.: Divergent surface and total soil moisture projections under global warming, Geophys. Res. Lett, 44, 236–244, https://doi.org/10.1002/2016gl071921, 2017.

Burrows, D.A., Ferguson, C.R., Campbell, M.A., Xia, G., Bosart, L.F.: An Objective Classification and Analysis of Upper-Level Coupling to the Great Plains Low-Level Jet over the Twentieth Century, J. Clim, 32, 7127–7152, https://doi.org/10.1175/jcli-d-18-0891.1, 2019.

Cheema, M.J.M., Bastiaanssen, W.G.M.: Land use and land cover classification in the irrigated Indus Basin using growth phenology information from satellite data to support water management analysis, Agric. Water Manag, 97, 1541–1552, https://doi.org/10.1016/j.agwat.2010.05.009, 2010.

Cheng, L., Hoerling, M.P., AghaKouchak, A., Livneh, B., Quan, X.-W., Eischeid, J.: How Has Human-Induced Climate Change Affected California Drought Risk?, J. Clim, 29, 111–120, https://doi.org/10.1175/jcli-d-15-0260.1, 2016.

Cheng, S., Guan, X., Huang, J., Fei Ji, Guo, R.: Long-term trend and variability of soil moisture over East Asia, J. Geophys. Res, 120, 8658–8670, https://doi.org/10.1002/2015jd023206, 2015.

https://doi.org/10.5194/egusphere-2025-625
Preprint. Discussion started: 5 March 2025

607 Chen, L., Ford, T. W., Yadav, P.: The role of vegetation in flash drought occurrence: a sensitivity
608 study using community earth system model, version 2, J. Hydrometeorol, 22, 845–57,
609 http://doi.org/10.1175/JHM-D-20-0214.1, 2021.

610 Christian, J.I., Basara, J.B., Hunt, E.D., Otkin, J.A., Xiao, X.: Flash drought development and
611 cascading impacts associated with the 2010 Russian heatwave, Environ. Res. Lett, 15, 094078,
612 https://doi.org/10.1088/1748-9326/ab9faf, 2020.

613 Christian, J.I., Basara, J.B., Otkin, J.A., Hunt, E.D.: Regional characteristics of flash droughts
614 across the United States, Environ. Res. Commun, 1, 125004, https://doi.org/10.1088/2515-
615 7620/ab50ca, 2019.

616 Dilling, L., Daly, M., Kenney, D., Klein, R., Miller, K.A., Ray, A.J., Travis, W.R., Wilhelmi, O.V.:
617 Drought in urban water systems: Learning lessons for climate adaptive capacity, Clim. Risk
618 Manag, 23, 32–42, https://doi.org/10.1016/j.crm.2018.11.001, 2019.

619 Dimri, A.P., Kumar, D., Chopra, S., Choudhary, A.: Indus River Basin: Future climate and water
620 budget, Int. J. Climatol, 39, 395–406, https://doi.org/10.1002/joc.5816, 2019.

621 Dorigo, W., Jeu, R., Chung, D., Parinussa, R., Liu, Y., Wagner, W., Fernández-Prieto, D.:
622 Evaluating global trends (1988–2010) in harmonized multi-satellite surface soil moisture,
623 Geophys. Res. Lett, 39, https://doi.org/10.1029/2012gl052988, 2012.

624 FAO (Food and Agriculture Organization of the United Nations).: Description of Four
625 Transboundary River Basins,
626 http://www.fao.org/nr/water/aquastat/countries_regions/asia_southeast/index.stm, 2011.

627 Fischer, E.M., Seneviratne, S.I., Lüthi, D., Schär, C.: Contribution of land-atmosphere coupling to
628 recent European summer heat waves, Geophys. Res. Lett, 34,
629 https://doi.org/10.1029/2006gl029068, 2007.

630 Ford, T.W., Labosier, C.F.: Meteorological conditions associated with the onset of flash drought
631 in the Eastern United States, Agric. For. Meteorol, 247, 414–423,
632 https://doi.org/10.1016/j.agrformet.2017.08.031, 2017.

633 Ford, T.W., McRoberts, D.B., Quiring, S.M., Hall, R.E.: On the utility of in situ soil moisture
634 observations for flash drought early warning in Oklahoma, USA, Geophys. Res. Lett, 42, 9790–
635 9798, https://doi.org/10.1002/2015gl066600, 2015.

636 Fu, Y.H., Zhao, H., Piao, S., Peaucelle, M., Peng, S., Zhou, G., Ciais, P., Huang, M., Menzel, A.,
637 Peñuelas, J., Song, Y., Vitasse, Y., Zeng, Z., Janssens, I.A.: Declining global warming effects on
638 the phenology of spring leaf unfolding, Nature, 526, 104–107,
639 https://doi.org/10.1038/nature15402, 2015.

https://doi.org/10.5194/egusphere-2025-625
Preprint. Discussion started: 5 March 2025

Gong, Z., Zhu, J., Li, T., Huang, D., Chen, X., Zhang, Q.: The features of regional flash droughts in four typical areas over China and the possible mechanisms, Sci. Total Environ, 154217–154217, https://doi.org/10.1016/j.scitotenv.2022.154217, 2022.

Gou, Q., Zhu, Y., Lü, H., Horton, R., Yu, X.u, Zhang, H., Wang, X., Su, J., Liu, E., Ding, Z., Wang, Z., Ren, L., , Yuan, F.: Application of an improved spatio-temporal identification method of flash droughts, J. Hydrol, 604, 127224, https://doi.org/10.1016/j.jhydrol.2021.127224, 2021.

Guo, W., Huang, S., Huang, Q., She, D., Shi, H., Leng, G., Li, J., Cheng, L., Gao, Y., Peng, J.: Precipitation and vegetation transpiration variations dominate the dynamics of agricultural drought characteristics in China, Sci. Total Environ, 898, 165480–165480, https://doi.org/10.1016/j.scitotenv.2023.165480, 2023.

Gupta, A., Rico-Medina, A., Caño-Delgado, A.I.: The physiology of plant responses to drought, Science, 368, 266–269, https://doi.org/10.1126/science.aaz7614, 2020.

Hattermann, F.F., Vetter, T., Breuer, L., Su, B., Daggupati, P., Donnelly, C., Fekete, B.M., Flörke, M., Seneviratne, S.I., Simon N. Gosling, Gosling, S.N., Hoffmann, P., Liersch, S., Masaki, Y., Motovilov, Y., Müller, C., Samaniego, L., Stacke, T., Wada, Y., Yang, T., Krysanova, V.: Sources of uncertainty in hydrological climate impact assessment: a cross-scale study, Environ. Res. Lett, 13, 015006, https://doi.org/10.1088/1748-9326/aa9938, 2018.

Hina, S., Saleem, F., Arshad, A., Hina, A., Ullah, I.: Droughts over Pakistan: possible cycles, precursors and associated mechanisms, Geomat. Nat. Hazards Risk, 12, 1638–1668, https://doi.org/10.1080/19475705.2021.1938703, 2021.

Hunt, E.D., Hubbard, K.G., Wilhite, D.A., Arkebauer, T.J., Dutcher, A.L.: The development and evaluation of a soil moisture index, Int. J. Climatol, 29, 747–759, https://doi.org/10.1002/joc.1749, 2009.

Hunt, E.D., Svoboda, M., Wardlow, B.D., Hubbard, K.G., Hayes, M.J., Arkebauer, T.J.: Monitoring the effects of rapid onset of drought on non-irrigated maize with agronomic data and climate-based drought indices, Agric. For. Meteorol, 191, 1–11, https://doi.org/10.1016/j.agrformet.2014.02.001, 2014.

Hu, C., She, D., Wang, G., Zhang, L., Jing, Z., Song, Z., Xia, J.: Unravelling spatiotemporal propagation processes among meteorological, soil, and evaporative flash droughts from a three-dimensional perspective, Agricultural Water Management, 308, 109294, https://doi.org/10.1016/j.agwat.2025.109294, 2025.

Immerzeel, W.W., Wanders, N., Lutz, A.F., Shea, J.M., Bierkens, M.F.P.: Reconciling high-altitude precipitation in the upper Indus basin with glacier mass balances and runoff, 19, 4673-4687, https://doi.org/10.5194/hess-19-4673-2015, 2016.

https://doi.org/10.5194/egusphere-2025-625
Preprint. Discussion started: 5 March 2025

674 Jafari, M., Kamali, H., Keshavarz, A., Keshavarz, A., Momeni, A.: Estimation of
675 evapotranspiration and crop coefficient of drip-irrigated orange trees under a semi-arid climate,
676 Agric. Water Manag, 248, 106769, https://doi.org/10.1016/j.agwat.2021.106769, 2021.

677 Janjua, S., Hassan, I., Shoaib, M., Ahmed, S., Ahmed, A.: Water management in Pakistan's Indus
678 Basin: challenges and opportunities, Water Policy, https://doi.org/10.2166/wp.2021.068, 2021.

679 JaSOn, A., Otkin, M. S., Hunt D., Ford, W., Martha, C., Hain, A.C.: FLASH DROUGHTS A
680 Review and Assessment of the Challenges Imposed by Rapid-Onset Droughts in the United States
681 Want to make a valuable contribution to your local library or community college?, Bulletin of
682 American Meteorological Society, 99, 911-919, https://doi.org/10.1175/BAMS-D-17-0149.1,
683 2018.

684 Jia, B., Liu, J., Xie, Xie, Zhenghui, Shi, C.: Interannual Variations and Trends in Remotely Sensed
685 and Modeled Soil Moisture in China, J. Hydrometeorol, 19, 831–847, https://doi.org/10.1175/jhm-
686 d-18-0003.1, 2018.

687 Khan, A.N., Khan, S.N.: Drought Risk and Reduction Approaches in Pakistan, Disaster Risk
688 Reduction, Springer, Tokyo, 131–143, https://doi.org/10.1007/978-4-431-55369-4_7, 2015.

689 Khan, S.U., Hasan, M.U.: Climate Classification of Pakistan, Int. J. Econ. Environ. Geol, 10, 60–
690 71, https://doi.org/10.46660/ijeeg.vol10.iss2.2019.264, 2019.

691 Koirala, S., Jung, M., Reichstein, M., Graaf, I.E.M., Camps-Valls, G., Ichii, K., Papale, D., Ráduly,
692 B., Schwalm, C.R., Tramontana, G., Carvalhais, N.: Global distribution of groundwater-vegetation
693 spatial covariation, Geophys. Res. Lett, 44, 4134–4142, https://doi.org/10.1002/2017gl072885,
694 2017.

695 Koster, R. D., Schubert, S.D., Wang, H., Mahanama, S., DeAngelis, A.M.: Flash Drought as
696 Captured by Reanalysis Data: Disentangling the Contributions of Precipitation Deficit and Excess
697 Evapotranspiration, J. Hydrometeorol, 20, 1241–1258, https://doi.org/10.1175/jhm-d-18-0242.1,
698 2019.

699 Krakauer, N.Y., Lakhankar, T., Dars, G.H.: Precipitation Trends over the Indus Basin, Climate, 7,
700 116, https://doi.org/10.3390/cli7100116, 2019.

701 Krishnan, R., Shrestha, A.B., Ren, G., Rajbhandari, R., Saeed, S., Sanjay, J., Syed, M.A., Vellore,
702 R., Xu, Y., You, Q., Ren, Y.: Unravelling Climate Change in the Hindu Kush Himalaya: Rapid
703 Warming in the Mountains and Increasing Extremes. Hindu Kush Himalaya Assessment, Springer,
704 Cham, 57–97, https://doi.org/10.1007/978-3-319-92288-1_3, 2019.

705 Kumar, M.R., Mishra, D.C., Singh, B.: Lithosphere, crust and basement ridges across Ganga and
706 Indus basins and seismicity along the Himalayan front, India and Western Fold Belt, Pakistan, J.
707 Asian Earth Sci, 75, 126–140, https://doi.org/10.1016/j.jseaes.2013.07.004, 2013.

https://doi.org/10.5194/egusphere-2025-625
Preprint. Discussion started: 5 March 2025

Laghari, A.N., Vanham, D., Rauch, W.: The Indus basin in the framework of current and future water resources management, Hydrol. Earth Syst. Sci, 16, 1063–1083, https://doi.org/10.5194/hess-16-1063-2012, 2012.

Lesinger, K., Tian, D.: Trends, Variability, and Drivers of Flash Droughts in the Contiguous United States, Water Resour. Res, 58, https://doi.org/10.1029/2022wr032186, 2022.

Liu, Y., Zhu, Y., Ren, L., Otkin, J.A., Hunt, E.D., Yang, X., Yuan, F., Jiang, S.: Two Different Methods for Flash Drought Identification: Comparison of Their Strengths and Limitations, J. Hydrometeorol, 21, 691–704, https://doi.org/10.1175/jhm-d-19-0088.1, 2020.

Li, J., Wu, C., Xia, C. A., Yeh, P. J. F., Chen, B., Lv, W., Hu, B. X.: A voxel-based three-dimensional framework for flash drought identification in space and time, Journal of Hydrology, 608, 127568, https://doi.org/10.1016/j.jhydrol.2022.127568, 2022.

Lutz, A.F., Immerzeel, W.W., Kraaijenbrink, P.D.A., Shrestha, A.B., Bierkens, M.F.P.: Climate Change Impacts on the Upper Indus Hydrology: Sources, Shifts and Extremes, PloS One, 11.11, e0165630, https://doi.org/10.1371/journal.pone.0165630, 2016.

Mahto, S.S., Mishra, V.: Dominance of summer monsoon flash droughts in India, Environ. Res. Lett, 15, 104061, https://doi.org/10.1088/1748-9326/abaf1d, 2020.

Mahto, S.S., Mishra, V.: Increasing risk of simultaneous occurrence of flash drought in major global croplands, Environ. Res. Lett, 18, 044044–044044, https://doi.org/10.1088/1748-9326/acc8ed, 2023.

Mishra, A.K., Singh, V.P.: A review of drought concepts, J. Hydrol, 391, 202–216, https://doi.org/10.1016/j.jhydrol.2010.07.012, 2010.

Mo, K.C., Lettenmaier, D.P.: Precipitation Deficit Flash Droughts over the United States, J. Hydrometeorol, 17, 1169–1184, https://doi.org/10.1175/jhm-d-15-0158.1, 2016.

Možný, M., Miroslav, T., Zalud, Z., Hlavinka, P., Nekovar, J., Potop, V., Virag, M.: Use of a soil moisture network for drought monitoring in the Czech Republic, Theor. Appl. Climatol, 107, 99–111, https://doi.org/10.1007/s00704-011-0460-6, 2012.

Mukherjee, S., Mishra, A.K.: Global flash drought analysis: uncertainties from indicators and datasets, Earth's Future, 10, https://doi.org/10.1029/2022ef002660, 2022.

Neelam, M., Hain, C.: Global Flash Droughts Characteristics: Onset, Duration, and Extent at Watershed Scales, Geophys. Res. Lett, 51, https://doi.org/10.1029/2024gl109657, 2024.

Nanditha, j.s., Kushwaha, A.P., Singh, R., Malik, I., Solanki, H., Chuphal, D.S., Dangar, S., Mahto, S.S., Vegad, U., Mishra, V.: The Pakistan Flood of August 2022: Causes and Implications, Earths Future, 11, https://doi.org/10.1029/2022ef003230, 2023.

https://doi.org/10.5194/egusphere-2025-625
Preprint. Discussion started: 5 March 2025

741 Noguera, I., Domínguez-Castro, F., Vicente-Serrano, S.M.: Characteristics and trends of flash
742 droughts in Spain, 1961-2018, Ann. N. Y. Acad. Sci, 1472, 155–172,
743 https://doi.org/10.1111/nyas.14365, 2020.

744 Osman, M.M., Mahmoud Osman, Zaitchik, B.F., Zaitchik, B.F., Hamada S. Badr, Badr, H.S.,
745 Christian, J.I., Tadesse, T., Otkin, J.A., Martha C. Anderson, Anderson, M.C.: Flash drought onset
746 over the contiguous United States: sensitivity of inventories and trends to quantitative definitions,
747 Hydrol. Earth Syst. Sci. Discuss, 25, 565–581, https://doi.org/10.5194/hess-2020-385, 2020.

748 Otkin, J.A., Anderson, M.C., Hain, C., Svoboda, M.: Examining the relationship between drought
749 development and rapid changes in the evaporative stress index, J. Hydrometeorol, 15, 938–956,
750 https://doi.org/10.1175/jhm-d-13-0110.1, 2014.

751 Otkin, J.A., Anderson, M.C., Hain, C., Svoboda, M., Johnson, D.K., Mueller, R., Tadesse, T.,
752 Wardlow, B.D., Brown, J.F.: Assessing the evolution of soil moisture and vegetation conditions
753 during the 2012 United States flash drought, Agric. For. Meteorol, 218219, 230–242,
754 https://doi.org/10.1016/j.agrformet.2015.12.065, 2016.

755 Otkin, J.A., Zhong, Y., Hunt, E.D., Basara, J.B., Svoboda, M., Anderson, M.C., Hain, C.:
756 Assessing the Evolution of Soil Moisture and Vegetation Conditions during a Flash Drought–Flash
757 Recovery Sequence over the South-Central United States, J. Hydrometeorol, 20, 549–562,
758 https://doi.org/10.1175/jhm-d-18-0171.1, 2019.

759 Otto, F. E., Zachariah, M., Saeed, F., Siddiqi, A., Shahzad, K., Mushtaq, H., et al.: Climate change
760 likely increased extreme monsoon rainfall, flooding highly vulnerable communities in Pakistan.
761 *Izidine Pinto*, *10*, 2022.

762 Park, S.K., Sungmin, O.: Flash drought drives rapid vegetation stress in arid regions in Europe,
763 Environ. Res. Lett, 18, 014028–014028, https://doi.org/10.1088/1748-9326/acae3a, 2023.

764 Peñuelas, J., Filella, I.: Responses to a Warming World, Science, 294, 793–795,
765 https://doi.org/10.1126/science.1066860, 2001.

766 Pendergrass, A.G., Meehl, G.A., Roger S. Pulwarty, R.S., Hobbins, M.T., Hoell, A.,
767 AghaKouchak, A., C. Bonfils, Gallant, A.J.E., Hoerling, M.P., Hoffmann, D., L. Kaatz, Lehner,
768 F., Llewellyn, D., Mote, P.W., Neale, R., Overpeck, J.T., Sheffield, A.M., Stahl, K., Svoboda, M.,
769 Wheeler, M.C., Wood, A.W., Woodhouse, C.A.: Flash droughts present a new challenge for
770 subseasonal-to-seasonal prediction, Nat. Clim. Change, 10, 191–199,
771 https://doi.org/10.1038/s41558-020-0709-0, 2020.

772 Perkins-Kirkpatrick, S.E., Lewis, S.C.: Increasing trends in regional heatwaves, Nat. Commun,
773 11, 3357, https://doi.org/10.1038/s41467-020-16970-7, 2020.

https://doi.org/10.5194/egusphere-2025-625
Preprint. Discussion started: 5 March 2025

774 Piao, S., Liu, Q., Liu, Q., Chen, A., Janssens, I.A., Fu, Y.H., Dai, J., Liu, L., Lian, X., Shen, M.,
775 Zhu, X.: Plant phenology and global climate change: Current progresses and challenges, Glob.
776 Change Biol, 25, 1922–1940, https://doi.org/10.1111/gcb.14619, 2019.

777 Potkay, A., Trugman, A.T., Wang, Y., Venturas, M., Anderegg, W.R.L., Caio R. C. Mattos,
778 Mattos, Fan, Y.: Coupled whole-tree optimality and xylem hydraulics explain dynamic biomass
779 partitioning, New Phytol, 230, 2226–2245, https://doi.org/10.1111/nph.17242, 2021.

780 Qing, Y., Wang, S., Yang, Z.L., Gentine, P., Zhang, B., Alexander, J.: Accelerated soil drying
781 linked to increasing evaporative demand in wet regions, Npj Clim. Atmospheric Sci, 6, 205,
782 https://doi.org/10.1038/s41612-023-00531-y, 2023.

783 Qing Y., Shuo, W., Shitong, W., Brian, C.A., Yang, ZL.: Accelerating flash droughts induced by
784 the joint influence of soil moisture depletion and atmospheric aridity, Nat. Commun, 13, 1139–
785 1139, https://doi.org/10.1038/s41467-022-28752-4, 2022.

786 Rahman, K.U., Shang, S., Balkhair, K.S., Nusrat, A.: Catchment-Scale Drought Propagation
787 Assessment in the Indus Basin of Pakistan Using a Combined Approach of Principal Components
788 and Wavelet Analyses, J. Hydrometeorol, 24, 601–624, https://doi.org/10.1175/jhm-d-22-0140.1,
789 2023.

790 Shah, J., Hari, V., Rakovec, O., Markonis, Y., Samaniego, L., Mishra, V., Hanel, M., Hinz, C.,
791 Kumar, R.: Increasing footprint of climate warming on flash droughts occurrence in Europe,
792 Environ. Res. Lett, 17, 064017, https://doi.org/10.1088/1748-9326/ac6888, 2022.

793 Shamsudduha, M., Panda, D.K.: Spatio-temporal changes in terrestrial water storage in the
794 Himalayan river basins and risks to water security in the region: A review, Int. J. Disaster Risk
795 Reduct, 35, 101068, https://doi.org/10.1016/j.ijdrr.2019.101068, 2019.

796 Shafeeque, M., Bibi, A.: Assessing the impact of future climate scenarios on crop water
797 requirements and agricultural water supply across different climatic zones of Pakistan, Front. Earth
798 Sci, 11, 1283171, https://doi.org/10.3389/feart.2023.1283171, 2023.

799 Shafeeque, M., Hafeez, M., Sarwar, A., Arshad, A., Khurshid, T., Asim, M., Ali, S., Dilawar, A.:
800 Quantifying future water-saving potential under climate change and groundwater recharge
801 scenarios in Lower Chenab Canal, Indus River Basin, Theor. Appl. Climatol, 155, 187-204,
802 https://doi.org/10.1007/s00704-023-04621-y, 2023.

803 Shafeeque, M., Luo, Y., Arshad, A., Muhammad, S., Ashraf, M., Pham, Q.: Assessment of climate
804 change impacts on glacio-hydrological processes and their variations within critical zone, Nat.
805 Hazards, 115, 2721-2748, https://doi.org/10.1007/s11069-022-05661-9, 2022.

806 Sheffield, J., Goteti, G., Wood, E.F.: Development of a 50-year high-resolution global dataset of
807 meteorological forcings for land surface modeling, J. Clim, 19, 3088–3111,
808 https://doi.org/10.1029/2002JD003274, 2006.

https://doi.org/10.5194/egusphere-2025-625
Preprint. Discussion started: 5 March 2025

Soares, P.M.M., Careto, J.A.M., Cardoso, R.M., Goergen, K., Trigo, R.M.: Land-Atmosphere Coupling Regimes in a Future Climate in Africa: From Model Evaluation to Projections Based on CORDEX-Africa, J. Geophys. Res, 124, 11118–11142, https://doi.org/10.1029/2018jd029473, 2019.

Sreeparvathy, V., Srinivas, V.: Meteorological flash droughts risk projections based on CMIP6 climate change scenarios, Npj Clim. Atmospheric Sci, 5, 77, https://doi.org/10.1038/s41612-022-00302-1, 2022.

Ting, M., Kushnir, Y., Seager, R., Li, C.: Forced and Internal Twentieth-Century SST Trends in the North Atlantic, J. Clim, 22, 1469–1481, https://doi.org/10.1175/2008jcli2561.1, 2009.

Ullah, I., S. Mukherjee., Syed, S., A. Mishra., B. Ayugi., Aadhar, S.: Anthropogenic and atmospheric variability intensifies flash drought episodes in South Asia, Commun. Earth Amp Environ, 5, 267, https://doi.org/10.1038/s43247-024-01390-y, 2024.

Hasson, S., and Böhner, J.: Hydrological Cycle Over the Indus Basin at Monsoon Margins: Present and Future, In Indus River Basin: Water Security and Sustainability, Elsevier, 245-264, https://:10.1016/B978-0-12-812782-7.00012-6, 2019.

Vinca, A., Parkinson, S., K. Riahi, Byers, E., Siddiqi, A., Muhammad, A., Ilyas, A., Yogeswaran, N., Willaarts, B., Magnuszewski, P., Awais, M., Rowe, A., Djilali, N.: Transboundary cooperation a potential route to sustainable development in the Indus basin, Nat. Sustain, 4, 331–339, https://doi.org/10.1038/s41893-020-00654-7, 2020.

Wang, L., Yuan, X.: Two Types of Flash Drought and Their Connections with Seasonal Drought, Adv. Atmospheric Sci, 35, 1478–1490, https://doi.org/10.1007/s00376-018-8047-0, 2018.

Wang, L., Yuan, X., Zhenghui, X., Wu, P., Li, Y.: Increasing flash droughts over China during the recent global warming hiatus, Sci. Rep, 6, 30571–30571, https://doi.org/10.1038/srep30571, 2016.

Western, A.W., Zhou, S.L., Grayson, R.B., McMahon, T.A., Blöschl, G., Wilson, D.J.: Spatial correlation of soil moisture in small catchments and its relationship to dominant spatial hydrological processes, J. Hydrol, 286, 113–134, https://doi.org/10.1016/j.jhydrol.2003.09.014, 2004.

Williams, A.P., Cook, E.R., Smerdon, J.E., Cook, B.I., Abatzoglou, J.T., Bolles, K., Baek, S.H., Livneh, B.: Large contribution from anthropogenic warming to an emerging North American megadrought, Science, 368, 314–318, https://doi.org/10.1126/science.aaz9600, 2020.

Xiang, Z., Yan, J., Demir, I.: A Rainfall-Runoff Model With LSTM-Based Sequence-to-Sequence Learning, Water Resour. Res, 56, https://doi.org/10.1029/2019wr025326, 2020.

Xia, Y., Hao, Z., Shi, C., Li, Y., Meng, J., Xu, T., Wu, X., Zhang, B.: Regional and global land data assimilation systems: innovations, challenges, and prospects, Journal of Meteorological Research, 33, 159–189, https://doi.org/10.1007/s13351-019-8172-4, 2019.

https://doi.org/10.5194/egusphere-2025-625
Preprint. Discussion started: 5 March 2025

Xu, Z., Wu, Z., He, H., Guo, X., Zhang, Y.: Comparison of soil moisture at different depths for drought monitoring based on improved soil moisture anomaly percentage index, Water Sci. Eng, 14, 171–183, https://doi.org/10.1016/j.wse.2021.08.008, 2021.

Xudong Z., Huang, S., Huang, S., Peng, J., Leng, G., Huang, Q., Fang, W., Guo, Y.: Flash Droughts Identification Based on an Improved Framework and Their Contrasting Impacts on Vegetation Over the Loess Plateau, China, Water Resour. Res, 58, https://doi.org/10.1029/2021wr031464, 2022.

Yang, L., Wang, W., Wei, J.: Assessing the response of vegetation photosynthesis to flash drought events based on a new identification framework, Agricultural and Forest Meteorology, 339, 109545, https://doi.org/10.1016/j.agrformet.2023.109545, 2023.

Yuan, X., Wang, L., Wu, P., Ji, P., Sheffield, J., Zhang, M.: Anthropogenic shift towards higher risk of flash drought over China, Nat. Commun, 10, 4661, https://doi.org/10.1038/s41467-019-12692-7, 2019.

Yuan, X., Wang, Y., Ji, P., Wu, P., Sheffield, J., Otkin, J. A., 2023. A global transition to flash droughts under climate change, Science, 380, 187-191, http://doi: 10.1126/science.abn6301, 2023.

Zeng, Z., Wu, W., Peñuelas, J., Li, Y., Jiao, W., Li, Z., Ren, X., Wang, K., Ge, Q.: Increased risk of flash droughts with raised concurrent hot and dry extremes under global warming, Npj Clim. Atmospheric Sci, 6, 134, https://doi.org/10.1038/s41612-023-00468-2, 2023.

Zheng, X., Huang, S., Jian, P., Guoyong, L., Qiang, H., Fang, W., Yi, G.: Flash Droughts Identification Based on an Improved Framework and Their Contrasting Impacts on Vegetation Over the Loess Plateau, China, Water Resour. Res, 58, https://doi.org/10.1029/2021wr031464, 2022.

Zhang, Y., You, Q., Chen, C., Li, X.: Flash droughts in a typical humid and subtropical basin: A case study in the Gan River Basin, China, J. Hydrol, 551, 162–176, https://doi.org/10.1016/j.jhydrol.2017.05.044, 2017.

Zhang, M., He, J., Wang, B., Wang, S., Li, S., Liu, W., Ma, X.: Extreme drought changes in Southwest China from 1960 to 2009, J. Geogr. Sci, 23, 3–16, https://doi.org/10.1007/s11442-013-0989-7, 2013.

Zhang, L., Liu, Y., Ren, L., Teuling, A.J., Zhu, Y., Wei, L., Zhang, L., Jiang, S., Yang, X., Fang, X., Yin, H.: Analysis of flash droughts in China using machine learning, Hydrol. Earth Syst. Sci, 26, 3241–3261, https://doi.org/10.5194/hess-26-3241-2022, 2022.

Zhou, S., A. Williams, A.P., Berg, A., Cook, B.I., Zhang, Y., Hagemann, S., Lorenz, R., Seneviratne, S.I., Gentine, P.: Land-atmosphere feedbacks exacerbate concurrent soil drought and atmospheric aridity, Proc. Natl. Acad. Sci. U. S. A, 116, 18848–18853, https://doi.org/10.1073/pnas.1904955116, 2019.

https://doi.org/10.5194/egusphere-2025-625
Preprint. Discussion started: 5 March 2025

879 Zhu, Q., Wang, Y.: The diagnosis about spatio-temporal characteristics and driving factors of flash
880 drought and its prediction over typical humid and semi-arid basins in China, J. Hydrometeorol, 22,
881 2783–2798, https://doi.org/10.1175/jhm-d-21-0062.1g2, 2021.

882

883

884